






Peripheral impairments of oxidative metabolism after a 10-day bed rest are upstream of mitochondrial respiration

Lucrezia Zuccarelli¹ , Giovanni Baldassarre¹, Benedetta Magnesa¹, Cristina Degano¹, Marina Comelli¹, Mladen Gasparini², Giorgio Manfredelli³, Mauro Marzorati³ , Irene Mavelli¹, Andrea Pilotto^{1,3} , Simone Porcelli^{3,4}, Letizia Rasica³, Boštjan Šimunič⁵, Rado Pišot⁵, Marco Narici⁶  and Bruno Grassi¹ 

¹Department of Medicine, University of Udine, Udine, Italy

²Splošna Bolnišnica Izola, Izola, Slovenia

³Institute of Biomedical Technologies, National Research Council, Milan, Italy

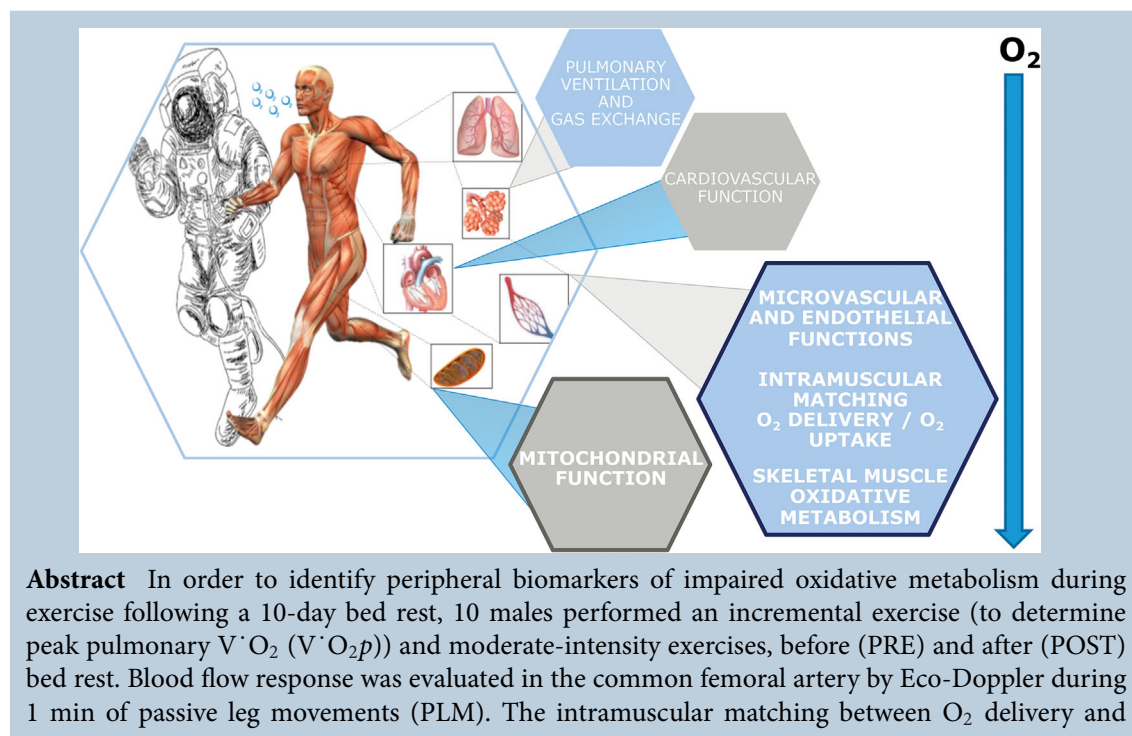
⁴Department of Molecular Medicine, University of Pavia, Pavia, Italy

⁵Institute of Kinesiology Research, Science and Research Centre, Koper, Slovenia

⁶Department of Biomedical Sciences, University of Padova, Padova, Italy

Edited by: Kim Barrett & Karyn Hamilton

The peer review history is available in the supporting information section of this article (<https://doi.org/10.1113/JP281800#support-information-section>).



Lucrezia Zuccarelli completed her BSc and MSc in Sport Science at the University of Milan. During her masters she was a visiting student at the European Space Agency in Cologne. She moved to Udine and completed her PhD in Biomedical Sciences at the University of Udine. Her research activity focuses on the functional evaluation of oxidative metabolism during exercise along the oxygen pathway from the ambient air to skeletal muscle mitochondria in physiological and non-physiological conditions.



O₂ utilization was evaluated by near-infrared spectroscopy (NIRS). Mitochondrial respiration was evaluated *ex vivo* by high-resolution respirometry in isolated muscle fibres, and *in vivo* by NIRS by the evaluation of skeletal muscle V̇O₂ (V̇O_{2m}) recovery kinetics. Resting V̇O_{2m} was estimated by NIRS. Peak V̇O_{2p} was lower in POST *vs.* PRE. The area under the blood flow *vs.* time curve during PLM was smaller ($P = 0.03$) in POST (274 ± 233 mL) *vs.* PRE (427 ± 291). An increased ($P = 0.03$) overshoot of muscle deoxygenation during a metabolic transition was identified in POST. Skeletal muscle citrate synthase activity was not different ($P = 0.11$) in POST (131 ± 16 nmol min⁻¹ mg⁻¹) *vs.* PRE (138 ± 19). Maximal ADP-stimulated mitochondrial respiration (66 ± 18 pmol s⁻¹ mg⁻¹ (POST) *vs.* 72 ± 14 (PRE), $P = 0.41$) was not affected by bed rest. Apparent K_m for ADP sensitivity of mitochondrial respiration was reduced in POST *vs.* PRE ($P = 0.04$). The V̇O_{2m} recovery time constant was not different ($P = 0.79$) in POST (22 ± 6 s) *vs.* PRE (22 ± 6). Resting V̇O_{2m} was reduced by 25% in POST *vs.* PRE ($P = 0.006$). Microvascular-endothelial function was impaired following a 10-day bed rest, whereas mitochondrial mass and function (both *in vivo* and *ex vivo*) were unaffected or slightly enhanced.

(Received 22 April 2021; accepted after revision 8 September 2021; first published online 10 September 2021)

Corresponding author B. Grassi: Department of Medicine, University of Udine, Piazzale Kolbe 4, 33100 Udine, Italy.
Email: bruno.grassi@uniud.it

Abstract figure legend Potential sites of impairment of oxidative metabolism during exercise following microgravity-inactivity.

Key points

- Ten days of horizontal bed rest impaired *in vivo* oxidative function during exercise.
- Microvascular impairments were identified by different methods.
- Mitochondrial mass and mitochondrial function (evaluated both *in vivo* and *ex vivo*) were unchanged or even improved (i.e. enhanced mitochondrial sensitivity to submaximal [ADP]).
- Resting muscle oxygen uptake was significantly lower following bed rest, suggesting that muscle catabolic processes induced by bed rest/inactivity are less energy-consuming than anabolic ones.

Introduction

It is well established that prolonged inactivity negatively affects almost all physiological systems (Booth *et al.* 2017). Bed rest studies offer a unique opportunity to evaluate the effects of prolonged muscle disuse and unloading, conditions experienced by bedridden patients with injuries and chronic diseases or by astronauts exposed to microgravity during spaceflight missions (Pavy-Le Traon *et al.* 2007). Exposure to microgravity or physical inactivity leads to impairment of oxidative metabolism, the main energy source for exercise or work activities lasting longer than 1–2 min. The impairment of oxidative metabolism during exercise is usually identified and quantified in terms of decreases in maximal or peak O₂ consumption (V̇O_{2peak}) (Ried-Larsen *et al.* 2017). However, the sites or functions responsible for this impairment are still debated. Whereas cardiovascular impairments, mainly represented by a decreased peak cardiac output (Q̇_{peak}) have been well described (see, e.g. Saltin *et al.* 1968; Ferretti *et al.* 1997; Porcelli

et al. 2010), peripheral (microvascular and mitochondrial) impairments appear to be more complex and somehow less defined.

Capelli *et al.* (2006) and Ferretti *et al.* (2009) utilized the multifactorial model of V̇O_{2max} limitation originally developed by di Prampero and Ferretti (1990), and concluded that the fractional limitation imposed by peripheral factors was about 30% after 42 days of bed rest, and about 40% after 90 days. More recent investigations reinforced the concept of peripheral factors as contributors to the decreased V̇O_{2peak} following microgravity exposure (Ade *et al.* 2015, 2017). Ade *et al.* (2015) utilized a two-component model originally proposed by Wagner *et al.* (1993), characterized by convective O₂ transport to the skeletal muscle capillary bed and by the diffusive O₂ transport from capillaries to mitochondria, and concluded that the decline in V̇O_{2peak} is initially (the first 10 days) mainly caused by a decrease in convective O₂ transport, whereas the role of diffusive O₂ transport increases with longer exposures. Salvadego *et al.* (2016, 2018) confirmed the presence of a peripheral impairment

of oxidative metabolism following bed rest by utilizing an experimental approach (dynamic knee extension of one limb) in which the reduced muscle mass significantly limits cardiovascular constraints (Richardson *et al.* 1993).

In terms of peripheral impairments, however, the respective roles of microvascular/endothelial function and mitochondrial respiration have not been systemically investigated. Porcelli *et al.* (2010) identified, following 35 days of bed rest, indirect signs of a mismatch between intramuscular O₂ delivery and O₂ uptake. The effects of shorter periods of bed rest on maximal mitochondrial respiration *ex vivo* are controversial. While Miotto *et al.* (2019) and Dirks *et al.* (2020) described an impaired mitochondrial function following bed rest periods of 3 and 7 days, respectively, other authors (Salvadeo *et al.* 2016; Larsen *et al.* 2018) did not see impairments following 4 and 10 days of bed rest exposure.

The general aim of the present study was to identify peripheral biomarkers of impairment of oxidative metabolism following a relatively short (10 days) exposure to horizontal bed rest, with specific attention toward the respective roles of microvascular/endothelial function and mitochondrial respiration. More specifically, we investigated microvascular/endothelial function by utilizing the passive leg movement (PLM) approach recently described by Gifford & Richardson (2017). By utilizing near-infrared spectroscopy (NIRS) (Grassi & Quaresima, 2016; Barstow 2019) we also looked for signs of impaired intramuscular matching between O₂ delivery and O₂ uptake (Porcelli *et al.* 2010, 2014, 2016; Grassi *et al.* 2019). We assessed mitochondrial function by utilizing two approaches, one *in vivo* (muscle $\dot{V}O_2$ recovery kinetics by NIRS and the repeated short occlusions method (Ryan *et al.* 2012; Adami & Rossiter, 2018; Zuccarelli *et al.* 2020)), and one *ex vivo* (mitochondrial respiration by high-resolution respirometry on permeabilized skeletal muscle fibres obtained by biopsy (Pesta & Gneiger, 2012)). From the analysis of the above-mentioned functional biomarkers we will be able to discriminate whether the peripheral limitations to oxidative metabolism are mainly upstream or at the level of mitochondrial function.

Methods

Ethical approval

This study was part of the Italian Space Agency (ASI) project 'MARS-PRE Bed Rest SBI 2019'. It was approved by the National Ethical Committee of the Slovenian Ministry of Health (ref. number: 0120-304/2019/9) and was performed in accordance with the standard set by the *Declaration of Helsinki*. All participants were informed about the aims, procedures and potential risks of the investigations before written consent was obtained.

Table 1. Anthropometric characteristics of participants before (PRE) and after (POST) a 10 day horizontal bed rest

	PRE	POST	P value
Height (m)	1.81 ± 0.04	1.82 ± 0.04	0.07
BM (kg)	77.5 ± 10.0	76.0 ± 19.4*	0.02
BMI (kg m ⁻²)	23.5 ± 2.5	23.0 ± 2.4*	0.009
Lean body mass (%)	80.9 ± 5.6	80.8 ± 6.0	0.74
Fat body mass (%)	19.1 ± 5.6	19.2 ± 6.0	0.74

Values are means ± SD. BM, body mass; BMI, body mass index.
*P < 0.05 different from PRE.

Subjects

Ten young, healthy, recreationally active males (age, 23 ± 5 yr; height, 1.81 ± 0.04 m; body mass (BM), 77.5 ± 10.0 kg; body mass index (BMI), 23.5 ± 2.5 kg m⁻²) participated in this study. Body mass composition was estimated in PRE and POST from data obtained by bioelectrical impedance analysis (Maltron 916s, UK). Participants' characteristics at baseline are given in Table 1. Subjects underwent a medical screening before the study. Exclusion criteria were: regular smoking, habitual use of drugs, blood clotting defects, history of deep vein thrombosis with D-dimer values >500 μg L⁻¹; acute or chronic skeletal, neuromuscular, metabolic and cardiovascular disease conditions, previous history of embolism, inflammatory diseases, psychiatric disorders, epilepsy, participation in sports at a competitive level and presence of ferromagnetic implants.

Experimental protocol

Each subject was evaluated before (PRE) and after (POST) 10 days of strict horizontal bed rest without countermeasures. The experiments were carried out at the Izola General Hospital, Slovenia. Participants arrived at the hospital 3 days before bed rest, and immediately after the PRE measurements were finished they entered the bed rest. POST measurements were carried out during the first 2 days after subjects arose from the bed. During bed rest no deviations from the lying position, muscle stretching or static contraction were allowed. Adherence to the assigned protocol was ensured using continuous closed-circuit television surveillance and constant supervision by researchers and medical staff. Subjects consumed an individually controlled, standardized diet and were allowed to drink water *ad libitum*. The dietary energy requirement was designed for each subject by multiplying resting energy expenditure (calculated by using the FAO/WHO equation and fat-free mass and fat mass data obtained by bioelectrical impedance (Müller *et al.* 2004)) by factors 1.2 and 1.4 in the bed rest and ambulatory periods, respectively (Biolo *et al.* 2008). The

macronutrient food content was set at 60% carbohydrates, 25% fats and 15% proteins.

The environmental conditions within the hospital remained stable throughout the experimental sessions. Before data collection, subjects were familiarized with the investigators, experimental arrangements and with the exercise protocols by means of short preliminary practice runs.

Both at PRE and POST the same schedule was followed. During baseline data collection day 1 (BDC1) subjects performed a PLM experimental session (see details below) for the evaluation of peripheral vascular and endothelial functions. PLM was followed by an incremental exercise (INCR) up to voluntary exhaustion on a cycle ergometer, for the determination of pulmonary $\dot{V}O_{2\text{peak}}$. During baseline data collection day 2 (BDC2) two repetitions of constant work rate cycling exercises of moderate intensity were performed. NIRS-obtained muscle oxygenation data at the onset of the constant work rate exercise were analysed in terms of the 'overshoot' of muscle deoxygenation, an indirect sign of a transient mismatch between intramuscular O_2 delivery and O_2 uptake (Porcelli *et al.* 2010, 2014, 2016; Grassi *et al.* 2019). During constant work rate exercise, muscle $\dot{V}O_2$ ($\dot{V}O_{2m}$) recovery kinetics and resting $\dot{V}O_{2m}$ were determined by NIRS by the repeated occlusions method (Ryan *et al.* 2012; Adami & Rossiter, 2018; Zuccarelli *et al.* 2020). A skeletal muscle biopsy was obtained from the vastus lateralis muscle for the evaluation of mitochondrial respiration by high-resolution respirometry during day 1 and day 10 of bed rest. Post-bed rest measurements were carried out on two sequential days immediately after day 10 of bed rest. Subjects remained in bed until the first day of data collection post-bed rest, and stayed in a wheelchair or in bed between the measurements performed on days 1 and 2 post-bed rest.

Femoral artery blood flow during passive leg movements

Blood flow in the common femoral artery was estimated by measurements of blood flow velocity and vessel diameter distally to the inguinal ligament, 2.0–2.5 cm proximally to the bifurcation of the superficial and deep femoral artery, by using an ultrasound system (Vivid IQ, General Electric Medical Systems, Milwaukee, WI, USA) with a linear array transducer operating at the imaging frequency of 9 MHz. Two-dimensional measurements of the arterial lumen were made from B-mode images in longitudinal view. Measurements of the vessel diameter were taken at the same time point in the cardiac cycle (peak of the R wave derived from the integrated ECG system). Blood flow velocities were collected with the sample volume covering more than

75% of the arterial lumen, and with the insonation angle always kept $<60^\circ$. Arterial blood flow was automatically calculated second by second by the software available in the ultrasound system (204.x.x, General Electric Medical Systems, Milwaukee, WI, USA), by multiplying arterial cross-sectional area and mean blood flow velocity.

Blood flow measurements were performed at rest and during 1 min of PLM of the right leg, following recently provided guidelines (Gifford & Richardson, 2017). The subjects remained seated with their legs extended and supported for 15 min before data collection. Resting Eco-Doppler data were recorded for 2 min, and were followed by measurements performed during 60 s of cyclical passive knee extension and flexion movements. The movements were performed across a 90° range of motion ($180^\circ-90^\circ-180^\circ$) at 1 Hz, following a metronome. The same trained researcher manually moved the subject's leg in PRE and in POST. The subjects were instructed not to activate their muscles during the movements. The absence of active movements was ensured during preliminary practice runs. The same researcher performed the Eco-Doppler measurements in PRE and in POST. Measurements were performed in duplicate, and the protocol was repeated after 15 min of recovery.

Measurements obtained during the two repetitions were superimposed and average values were obtained for each subject and retained for data analysis. Resting blood flow and peak blood flow during PLM were calculated. The area under the blood flow vs. time response (area under the curve, AUC) was obtained by calculating the integral of the function over the entire 60 s, after subtracting the resting baseline value (see Gifford & Richardson, 2017).

Intramuscular matching between O_2 delivery and O_2 utilization

Oxygenation changes in four different sites of the anterior compartment (vastus lateralis and rectus femoris muscles) of the right thigh were determined by a portable continuous-wave NIRS instrument (OctaMon M; Artinis Medical System, The Netherlands). In the present study only the data related to the probe positioned on the lower third of the vastus lateralis muscle are presented. The skin overlying the investigated muscle region was carefully shaven before the experimentation, and the place where the probe was attached was recorded using a skin marker; this allowed the apposition of the probe in the same position during all tests. Adipose tissue thickness (ATT) at the site of application of the NIR probe was determined by a caliper (Gima, Milan, Italy). Black bandages were put around the probe and the skin to prevent contamination from ambient light. The sampling frequency was set at 10 Hz. The light transmitter

(which emitted two wavelengths of 760 and 850 nm) was separated by 35 mm from the respective receiving optode. The instrument measures non-invasively micromolar (μM) changes in oxygenated haemoglobin (Hb) + myoglobin (Mb) concentrations ($\Delta[\text{oxy}(\text{Hb}+\text{Mb})]$) and in deoxygenated [Hb+Mb] ($\Delta[\text{deoxy}(\text{Hb}+\text{Mb})]$), with respect to an initial value arbitrarily set equal to zero and obtained during the resting condition preceding the exercise. The sum of the two variables ($\Delta[\text{total}(\text{Hb}+\text{Mb})]$) reflects changes in total Hb+Mb volume in the muscle region of interest. An increased $\Delta[\text{deoxy}(\text{Hb}+\text{Mb})]$ indicates an increased fractional O_2 extraction in the tissue under consideration (Grassi & Quaresima, 2016). The $\Delta[\text{deoxy}(\text{Hb}+\text{Mb})]$ signal was considered in the present study since it is usually less affected (with respect to the $\Delta[\text{oxy}(\text{Hb}+\text{Mb})]$ signal) by changes in blood volume in the tissue (Grassi & Quaresima, 2016).

The presence of a deoxygenation 'overshoot' (transitory sharp increase in $[\text{deoxy}(\text{Hb} + \text{Mb})]$ above the steady state (Grassi & Quaresima, 2016)) was investigated during the first 90 s of constant work rate exercise (Salvadeo *et al.* 2011; Porcelli *et al.* 2016; Salvadeo *et al.* 2018).

Data were fitted by a double exponential function of the type:

$$y(t) = y_{\text{bas}} + A_{\text{u}} [1 - e^{-(t-\text{TD}_{\text{u}})/\tau_{\text{u}}}] + A_{\text{d}} [1 - e^{-(t-\text{TD}_{\text{d}})/\tau_{\text{d}}}] \quad (1)$$

In eqn (1) y_{bas} indicates the baseline, A_{u} the amplitude of the upward component observed after 10–20 s of exercise, TD_{u} is the time delay and τ_{u} is the time constant of the upward component of the function (see Fig. 2). A_{d} , TD_{d} and τ_{d} indicate, respectively, the amplitude, time delay and time constant of the following downward (d) component. The muscle deoxygenation overshoot was calculated as the difference between the peak of the upward component and the asymptote of the downward component.

Mitochondrial respiration *in vivo*

During the recovery from the constant work rate cycling exercise mitochondrial respiration was evaluated *in vivo* by determining the $\dot{V}\text{O}_2m$ kinetics by NIRS and the repeated occlusions method (Ryan *et al.* 2012; Adami & Rossiter, 2018; Zuccarelli *et al.* 2020). The NIRS instrument and the site of application of the NIRS probe were the same described above. The NIRS signals during ischaemia were normalized for changes in blood volume by utilizing the method proposed by Ryan *et al.* (2012). Before the exercise period a 5 min ischaemic calibration (physiological normalization) was performed by inflating a pressure cuff (~ 300 mmHg) positioned at the inguinal crease of the thigh.

$\dot{V}\text{O}_2m$ was estimated by calculating the slope of the initial (3 s) linear increase in NIRS-measured $\Delta[\text{deoxy}(\text{Hb} + \text{Mb})]$ during short (5 s) bouts of ischaemia induced by rapid (less than 1 s) inflation and deflation of a pneumatic cuff (~ 300 mmHg) (Hokanson E20 cuff inflator, Bellevue, WA, USA) during the recovery from moderate-intensity constant work rate exercise (Zuccarelli *et al.* 2020). When muscle reached a deoxygenation target of 50% of the physiological normalization (Adami *et al.* 2017) (see above), several intermittent arterial occlusions were performed: the first five occlusions lasted 5 s each and were separated by 5 s; they were followed by five occlusions lasting 5 s each and separated by 10 s, and finally by five occlusions lasting 5 s and separated by 20 s. When the target 50% was not reached at the end of the exercise protocol the first arterial occlusion was performed after 5–10 s.

$\dot{V}\text{O}_2m$ values were then fitted by a monoexponential function according to eqn (2) (Ryan *et al.* 2014):

$$y(t) = y_{\text{END}} - \Delta \times e^{-t/\tau} \quad (2)$$

where $y(t)$ represents the value of $\dot{V}\text{O}_2m$ at a given time (t), y_{END} the $\dot{V}\text{O}_2m$ immediately after the cessation of the exercise, Δ is the change in $\dot{V}\text{O}_2m$ from rest to end exercise and τ is the rate constant ($k = [1/\tau]$, expressed in min^{-1}) of the function.

Resting $\dot{V}\text{O}_2m$ was estimated by calculating a linear regression of the $\Delta[\text{deoxy}(\text{Hb} + \text{Mb})]$ increases during the first 60 s of the physiological normalization procedure (see above). Also in this case the NIRS signals during ischaemia were normalized for changes in blood volume by utilizing the method proposed by Ryan *et al.* (2012).

Mitochondrial respiration *ex vivo*

Skeletal muscle biopsies were obtained from the vastus lateralis muscle under local anaesthesia (2% lidocaine). The biopsy was taken immediately before and at the end of the bed rest intervention. Following the application of the anaesthetic, a 1.0–1.5 cm incision was made to the skin, subcutaneous tissue and muscle fascia, and the tissue sample was harvested with a Rongeur-Conchotome (GmbH&Co, Zepf Instruments, Dürbheim, Germany). The collected muscle tissue was dissected free of fat and connective tissue and rapidly divided into several portions. A small portion (2.0–6.5 mg wet weight) was used immediately to evaluate mitochondrial respiration *ex vivo* (Pesta & Gnaiger 2012). Measurements were performed in duplicate. The portion of tissue was immediately placed in an ice-cold preservation solution (BIOPS; Oroboros Instruments, Innsbruck, Austria) (4°C) containing: EGTA-calcium buffer (10 mM) (free Ca^{2+} concentration $100 \text{ nmol}\cdot\text{L}^{-1}$), imidazole (20 mM), taurine (20 mM), $\text{K}^+/\text{4}$ morpholinoethanesulphonic acid

(50 mM), dithiothreitol (0.5 mM), MgCl₂ (6.56 mM), ATP (5.77 mM) and phosphocreatine (15 mM) (pH 7.1). Fibre bundles were trimmed from the connective and fat tissue excess (if present) and separated with sharp-ended needles under magnification (70×) (Stereomicroscope CRYSTAL-PRO, Konus-optical & sports systems, Italy). After this, fibre bundles were incubated into 2 mL of BIOPS containing 20 μg mL⁻¹ saponin for 30 min at 4°C with continuous gentle stirring to ensure complete permeabilization. Samples were washed with the respiration medium (MIR05; Oroboros Instruments, Innsbruck, Austria) containing 0.5 mM EGTA, 60 mM potassium lactobionate, 3 mM MgCl₂ 6H₂O, 20 mM taurine, 10 mM KH₂PO₄, 20 mM Hepes, 110 mM sucrose and 1 g L⁻¹ BSA, pH 7.1, weighed in a balance-controlled scale (Shimatzdu). After this, permeabilized fibres were measured for wet weight and immediately transferred into the respirometer (Oxygraph-2k Oroboros Instruments) chambers for O₂ consumption analysis. Mitochondrial respiratory function was evaluated by measuring O₂ consumption polarographically by high-resolution respirometry (Pesta & Gnaiger 2012). Data were digitally recorded using DatLab4 software (Oroboros Instruments). The instrumentation allows for O₂ consumption measurements with small amounts of sample in closed respiration chambers containing 2 mL of air-saturated respiration medium (MIR06; MIR05 + catalase 280 IU mL⁻¹) at 37°C. Standardized instrumental and chemical calibrations were performed to correct for back-diffusion of O₂ into the chamber from the various components (e.g. leak from the exterior, O₂ consumption by the chemical medium and by the sensor O₂) (Pesta & Gnaiger 2012). The O₂ concentration in the chamber was maintained between 280 and 400 μM (average O₂ partial pressure 250 mmHg) to avoid O₂ limitation of respiration. Intermittent reoxygenation steps were performed during the experiments by injections of 1–3 μL of 0.3 mM H₂O₂, which was instantaneously dismutated by catalase, already present in the medium, to O₂ and H₂O. Experiments were performed in the presence of the myosin II-ATPase inhibitor (Blebbistatin, 25 μM, dissolved in DMSO 5 mM stock) (Perry et al. 2011) in order to prevent spontaneous contraction in the respiration medium.

A substrate-uncoupler-inhibitor-titration protocol, with a substrate combination that matches physiological intracellular conditions, was applied (Pesta & Gnaiger 2012; Salvadego et al. 2016, 2018). Non-phosphorylating resting mitochondrial respiration was measured in the presence of malate (4 mM) and glutamate (10 mM) and in the absence of adenylates, so that O₂ consumption was mainly driven by the back leakage of protons through the inner mitochondrial membrane ('leak' respiration). Succinate (10 mM) was added to support convergent electron flow into the Q-junction through complexes I and II. This was followed by submaximal titration of

ADP (12.5, 25, 175, 250, 500, 1000, 2000, 4000, 6000, 8000, 10,000 μM) to assess complex I+II-linked ADP sensitivity and maximal ADP-stimulated mitochondrial respiration (OXPHOS). Cytochrome C (10 μM) was added to test mitochondrial outer membrane integrity. The addition of cytochrome C had no significant additive effects on respiration, with minor increases of <5%, thereby confirming the integrity of the outer mitochondrial membrane. Maximal uncoupled mitochondrial respiration (electron transport system capacity) was measured by stepwise additions of chemical uncoupler protonophore carbonylcyanide-p-trifluoromethoxyphenylhydrazone (FCCP). Rotenone (1 μM) and antimycin A (2.5 μM) were added to inhibit complexes I and III, providing a measure of residual O₂ consumption, indicative of non-mitochondrial O₂ consumption. Mitochondrial respiration indices were then corrected for O₂ flux resulting from residual O₂ consumption. The degree of coupling of oxidative phosphorylation for a specific substrate supply (glutamate and malate and succinate) was determined by calculating the ratio between OXPHOS and LEAK respiration (Pesta & Gnaiger 2012). The obtained mitochondrial respiration values were also normalized by citrate synthase activity (see below), taken as an estimate index of mitochondrial mass (Larsen et al. 2012).

In order to evaluate the sensibility of mitochondrial respiration to submaximal [ADP] (squared brackets denote concentrations) (Holloway et al. 2018), high-resolution respirometry was used to assess mitochondrial respiration, after giving glutamate, malate and succinate, in the presence of 11 increasing [ADP] (see above). ADP-stimulated respiration values (expressed as a percentage of the maximal values) were analysed by a Michaelis-Menten kinetic equation (eqn (3)):

$$y = V_{\max} [x / (K_m + x)] \quad (3)$$

where x is the [ADP] (μM), y indicates the mitochondrial respiration (O₂ consumption) at the given [ADP], V_{\max} is the maximal O₂ consumption and K_m is the [ADP] providing 50% of the maximal mitochondrial respiration.

Data were also fitted by a biexponential function according to eqn (4):

$$y(x) = y_{\text{BAS}} + A_1 \left[1 - e^{-(x-C_1)/CI_1} \right] + A_2 \left[1 - e^{-(x-C_2)/CI_2} \right] \quad (4)$$

where x is [ADP] (μM), y_{BAS} indicates the baseline, which was always set to 0, A_1 is the amplitude between the y_{BAS} and the steady state during the first exponential component, C_1 is the [ADP] at the beginning of the first exponential component, which was always set to 0, and CI_1 is the constant of increase that indicates the [ADP] needed to achieve 63% of the steady state during the

first exponential component. A_2 , C_2 and CI_2 indicate the amplitude of the second exponential component, the [ADP] at the start of the second exponential component and the constant of increase of the second exponential component, respectively. A variable equivalent to the apparent K_m (see above) was then calculated by solving eqn (4) in order to determine the [ADP] corresponding to 50% of the maximal ADP-stimulated mitochondrial respiration.

At the conclusion of each experiment, muscle samples were removed from the chamber, immediately frozen in liquid nitrogen and then stored at -80°C until determination of citrate synthase (CS) activity (see below).

Citrate synthase activity

In order to determine CS activity, muscle samples were thawed and underwent a motor-driven homogenization in a pre-cooled 1 mL glass-glass potter (Wheaton, USA). The muscle specimen was suspended 1:50 w/v in a homogenization buffer containing sucrose (250 mM), Tris (20 mM), KCl (40 mM) and EGTA (2 mM) with 1:50 v/v protease (P8340-Sigma) inhibitors. The specimen was homogenized in an ice-bath with 20 strokes at 500 rpm; before the last hit Triton X-100 (0.1% v/v) was added to the solution. After this, the sample was left in ice for 30 min. The homogenate was centrifuged at 14,000 g for 10 min. The supernatant was used to evaluate protein concentration according to the method of Lowry *et al.* (1951). Protein extracts (5–10–15 μg) were added to each well of a 96-well-microplate along with 100 μl of 200 mM Tris, 20 μl of 1 mM 5, 5'-dithiobis-2-nitrobenzoate (DTNB), freshly prepared, 6 μl of 10 mM acetyl-coenzyme A (Acetyl-Co-A) and mQ water to a final volume of 190 μl . A background ΔAbs , to detect any endogenous activity by acetylase enzymes, was recorded for 90 s with 10 s intervals at 412 nm at 25°C by an EnSpire 2300 Multilabel Reader (PerkinElmer). The ΔAbs was subtracted from the one given after the addition of 10 μl of 10 mM oxalacetic acid that started the reaction. All assays were performed at 25°C in triplicate on homogenates. Activity was expressed as nmol min^{-1} (mU) per mg of protein. This protocol was modified from (Sreer 1969; Spinazzi *et al.* 2012).

Statistical analysis

Data are presented as means \pm SD with the exception of Fig. 1 where SEM is used for clarity. Statistical significance of differences between POST and PRE was checked by a two-tailed Student's t test for paired data. The level of significance was set at $P < 0.05$. Data fittings by exponential functions were performed by the least-squared residuals method. Statistical analyses

were carried out with a commercially available software package (Prism 6.0; GraphPad).

Results

Each subject completed the entire experimental protocol. Pulmonary $\dot{V}\text{O}_{2\text{peak}}$ was 9% lower in POST ($40.3 \pm 6.1 \text{ ml}\cdot\text{kg}^{-1} \text{ min}^{-1}$) vs. PRE (44.5 ± 7.2) ($P = 0.001$). Anthropometric characteristics are reported in Table 1. BM and BMI decreased by $\sim 2\%$ after bed rest. Skin and ATT measured at the site of placement of the NIRS probe ranged between 4.0 and 8.4 mm; the thickness was slightly reduced after bed rest ($P = 0.03$).

Femoral artery blood flow during passive leg movements

Baseline blood flow in the common femoral artery was not affected by bed rest ($443 \pm 100 \text{ mL min}^{-1}$ in POST vs. 429 ± 96 in PRE; $P = 0.55$). On the contrary, baseline common femoral artery diameter was reduced after bed rest, by about 5% ($0.89 \pm 0.11 \text{ cm}$ in POST vs. 0.94 ± 0.12 in PRE; $P = 0.02$). The PLM results are presented in Fig. 1. Leg blood flow increased immediately after the onset of PLM, reaching a peak both in PRE ($1310 \pm 467 \text{ mL min}^{-1}$) and in POST (1107 ± 472) after about 10 s. Peak blood flow values in the two conditions were not significantly different ($P = 0.19$). The area under the blood flow vs. time curve (AUC) during PLM was smaller ($P = 0.03$) in POST ($274 \pm 233 \text{ mL}$) vs. PRE (427 ± 291).

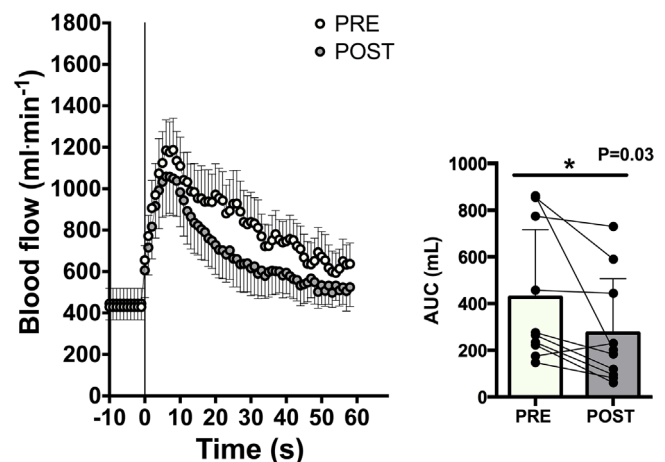


Figure 1. Passive leg movement responses

In the left panel, mean values of blood flow in the common femoral artery at rest and in response to passive leg movement (PLM), before (PRE) and after (POST) 10 days of bed rest are shown. The vertical line indicates the onset of PLM. Data are presented as means \pm SEM. In the right panel, individual and mean values of the area under the curve (AUC) in response to PLM are given. Data are presented as means \pm SD. * indicates the presence of a statistically significant difference. See text for further details. [Colour figure can be viewed at wileyonlinelibrary.com]

Intramuscular matching between O₂ delivery and O₂ utilization

The upper panels of Fig. 2 show [deoxy(Hb + Mb)] values of a typical subject in PRE and in POST during the first 90 s of very low-intensity exercise, corresponding to about 30 W. An 'overshoot' (see *Methods*) of [deoxy(Hb + Mb)] was evident in the majority of the subjects both in PRE (7 out of 10) and in POST (9 out of 10). The individual and mean (\pm SD) values of the amplitude of the overshoot are given in the lower panel of Fig. 2. The amplitude was greater ($P = 0.03$) in POST vs. PRE.

Mitochondrial respiration *in vivo*

Representative repeated arterial occlusion protocols in PRE and POST are shown in Fig. 3. $\dot{V}O_{2m}$ recovery curves for a typical subject in PRE and in POST are shown in the upper panels of Fig. 4. A monoexponential decrease was observed for all participants. For all experiments the fitting was excellent, and the coefficients of determination (r^2) ranged between 0.90 and 0.95. Individual and mean (\pm SD) values of τ (time constant) and k (velocity constant) of the $\dot{V}O_{2m}$ recovery kinetics are shown in the lower panels of Fig. 4. No significant differences of data obtained in POST vs. PRE were observed. In other words, bed rest did not affect the $\dot{V}O_{2m}$ recovery kinetics (see Fig. 4).

The dashed horizontal lines in the upper panels indicate the $\dot{V}O_{2m}$ values obtained at rest before the exercise. Resting $\dot{V}O_{2m}$ values were lower than the asymptotic $\dot{V}O_{2m}$ values obtained with the fitting; in other words, at the end of the repeated arterial occlusions, $\dot{V}O_{2m}$ still did not reach the resting values. Δ [deoxy(Hb + Mb)] values during the first occlusion following the exercise were about 30% of the physiological calibration. $\dot{V}O_{2m}$ values extrapolated at time = 0 (start of the recovery) in the upper panel of Fig. 4 were about 48 and 37 times higher in POST and in PRE, respectively, than resting $\dot{V}O_{2m}$.

Mean linear regression lines of the Δ [deoxy(Hb + Mb)] increases during the first minute of the blood occlusion manoeuvres performed for the 'physiological calibration' (see above) are presented in the upper panel of Fig. 5. Resting $\dot{V}O_{2m}$ values (see individual and mean (\pm SD) values in the lower panel of Fig. 5) were about 25% lower in POST ($0.057 \pm 0.02 \mu\text{M s}^{-1}$) vs. PRE (0.078 ± 0.02) ($P = 0.006$).

Mitochondrial respiration *ex vivo*

Individual and mean (\pm SD) data of CS activity are shown in Fig. 6. No significant differences were observed in POST vs. PRE. Being aware of the potential problem of determining CS activity in a very small muscle bundle (max 6.5 mg wet weight) which for ~ 1 –1.5 h

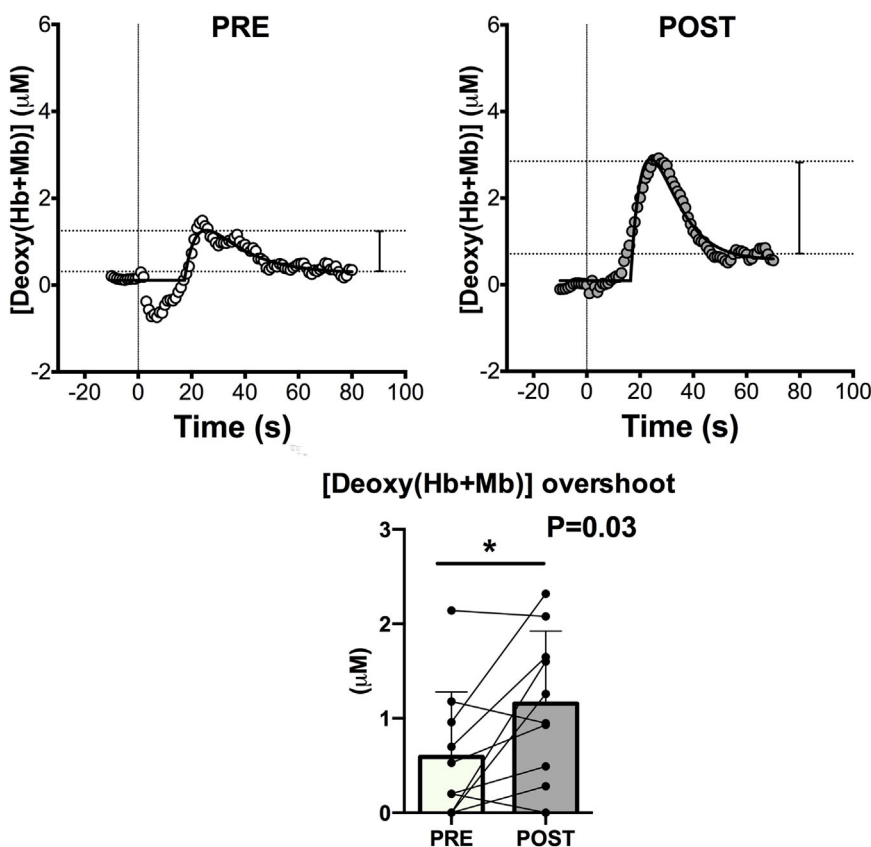


Figure 2. Intramuscular matching between O₂ delivery and O₂ utilization In the upper panels, typical examples of the dynamics of [deoxy(Hb+Mb)] during the first 60 s of constant work rate cycling exercise are shown before (PRE, left panel) and after (POST, right panel) bed rest. The presence of a transient deoxygenation overshoot was checked by fitting the responses by two exponential equations (see *Methods*) (solid line). The amplitude of the overshoot is indicated by vertical distance between the asymptotes of the two equations (indicated by the horizontal dashed lines). In the lower panel, individual and mean (\pm SD) values of the overshoot data before (PRE) and after (POST) bed rest are shown. * indicates the presence of a statistically significant difference. See text for further details. [Colour figure can be viewed at wileyonlinelibrary.com]

was kept at 37°C for the respiratory measurements, we performed pilot experiments (unpublished observations) in which we compared CS measurements determined on samples taken from the same muscle but undergoing two different procedures: in one case the CS measurements were performed (as in the present study) on material frozen after it was taken from the chamber following the respirometry experiments, whereas in the ‘control’ condition, the CS measurements were performed on samples immediately frozen after the biopsy. The results did not show significant differences between the two measurements: $410 \pm 50 \text{ nmol min}^{-1} \text{ mg protein vs. } 390 \pm 50$, $n = 10$, $P = 0.23$.

The main data related to mitochondrial respiration ($\dot{V}O_2$) *ex vivo* obtained by high-resolution respirometry are presented in Fig. 6. The data were expressed per mg of wet weight. Although there were inter-individual variations in the responses to bed rest, for all variables there were no significant changes in POST vs. PRE. Mitochondrial leak respiration (‘LEAK’), maximal ADP-stimulated mitochondrial respiration (‘OXPHOS’), supported by complex I and complex II, and the maximal uncoupled mitochondrial respiration supported by complex I and complex II (‘ETS’) were not significantly

different in POST vs. PRE. Also rotenone-insensitive ETS, the mitochondrial electron transport system capacity supported by complex II, was not significantly different ($P = 0.09$) in PRE ($46.6 \pm 13.2 \text{ pmol s}^{-1} \text{ mg}^{-1}$) vs. POST (38.6 ± 10.4).

The general message (no significant differences in mitochondrial respiration variables in POST vs. PRE) was confirmed after LEAK, OXPHOS and ETS respiration values were normalized per unit of CS activity. LEAK/CS was $0.149 \pm 0.054 \text{ pmol s}^{-1} \text{ mU}^{-1}$ in POST and 0.140 ± 0.055 in PRE ($P = 0.67$); OXPHOS/CS was $0.509 \pm 0.134 \text{ pmol s}^{-1} \text{ mU}^{-1}$ in POST and 0.534 ± 0.135 in PRE ($P = 0.61$) and ETS/CS was $0.485 \pm 0.161 \text{ pmol s}^{-1} \text{ mU}^{-1}$ in POST and 0.579 ± 0.158 in PRE ($P = 0.14$).

Also, the mitochondrial coupling of oxidative phosphorylation (‘respiratory control ratio’), calculated by the ratio OXPHOS/LEAK was not significantly different in POST vs. PRE (see Fig. 6; $P = 0.44$). The ratio between OXPHOS and ETS (‘respiratory system control ratio’) was significantly higher in POST compared with PRE (see Fig. 6). In PRE, ETS capacity was slightly but significantly

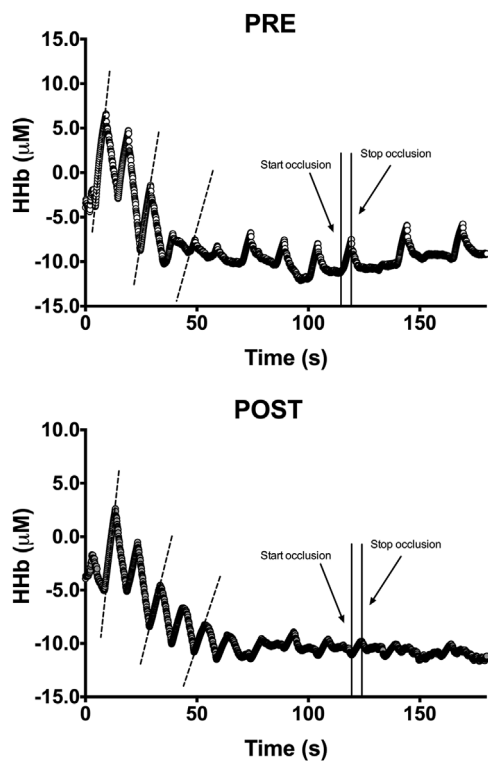


Figure 3. Repeated arterial occlusion protocol

Typical examples of the changes in [deoxy(Hb+Mb)] values during the first 12 ischaemia before (PRE, upper panel) and after bed rest (POST, lower panel). Dashed lines represent the recovery of muscle $\dot{V}O_2$ over time.

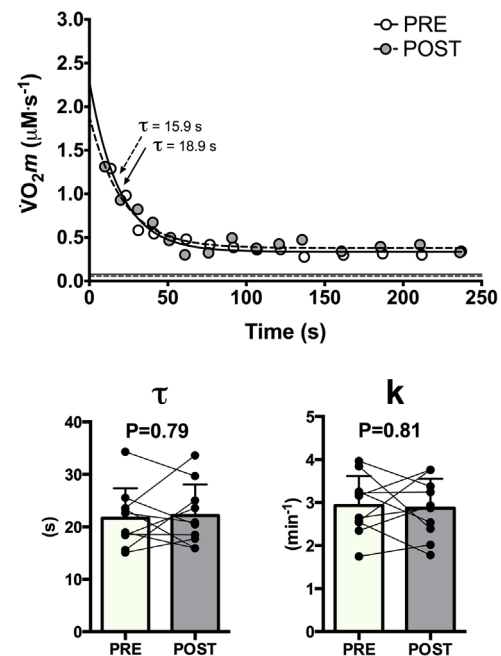


Figure 4. Assessment of *in vivo* mitochondrial function

In the upper panel, muscle $\dot{V}O_2$ ($\dot{V}O_{2m}$) data during the recovery from moderate-intensity exercise are shown for a representative subject before (PRE) and after (POST) bed rest. The inset shows mitochondrial respiration in response to the first ADP titrations. The fitted functions and the calculated time constant (τ) values (see *Methods*) are also shown. The dotted horizontal lines indicate the resting baseline values. In the lower panel, individual and mean (\pm SD) values of the time constant and rate constant (k) of muscle $\dot{V}O_2$ ($\dot{V}O_{2m}$) recovery kinetics before (PRE) and after (POST) bed rest are shown. No statistically significant differences were observed. See text for further details. [Colour figure can be viewed at wileyonlinelibrary.com]

higher than OXPHOS (+8%; $P = 0.01$), indicating that the phosphorylating system exerted a control over coupled respiration (Pesta & Gnaiger 2012). This control disappeared after bed rest (+0% between ETS capacity and OXPHOS; $P = 0.36$) (see Fig. 6).

High-resolution respirometry was also used to assess the sensitivity of mitochondrial respiration to submaximal [ADP] (Holloway *et al.* 2018). Data were first analysed according to Michaelis–Menten kinetics (see *Methods*), as previously described (see, e.g. Perry *et al.* 2011; Holloway *et al.* 2018). The upper panel of Fig. 7 shows a typical example of the ADP-stimulated respiration data fitted by this approach. Although the coefficient of determination (r^2) was relatively high (0.83), the fitting was obviously not satisfying. Analysis of residuals (see inset panels) shows that the fitting markedly overestimates JO_2 data from 1000 to 2000 μM , and markedly underestimates JO_2 data from 6000 to 10,000 μM . The same typical example was fitted with a double exponential model (see eqn (4) and lower panel of Fig. 7) and the quality of the fitting markedly

improved, as also confirmed by the analysis of residuals (see also the *Discussion*).

We therefore opted for the second fitting approach, and the fittings performed on the mean JO_2 values are shown for PRE and POST in Fig. 8. The high quality of the fitting was confirmed. A greater sensitivity of JO_2 to submaximal [ADP] in POST *vs.* PRE is evident from the figure: for the same submaximal [ADP], higher JO_2 values are present in POST. Equation (3) was then applied to the individual values, and the equations were solved in order to calculate the [ADP] values corresponding to 50% of maximal JO_2 . This parameter should have the same meaning of the K_m obtained with the classic Michaelis–Menten equation. [ADP] at 50% of JO_2 max was significantly lower in POST *vs.* PRE (see individual and mean (\pm SD) values in the lower panel of Fig. 8), confirming the increased sensitivity of JO_2 to submaximal [ADP] in POST *vs.* PRE.

Discussion

The general aim of the present study was to identify peripheral biomarkers of impairment of oxidative metabolism during exercise following a relatively short (10 days) exposure to horizontal bed rest, with specific attention toward the respective roles of microvascular–endothelial function and mitochondrial respiration. The main sites of impairment were located upstream of mitochondria, at the level of microvascular and endothelial functions and in the intramuscular matching between O_2 delivery and O_2 uptake, whereas mitochondrial mass estimated only *ex vivo* and respiratory activity, both *in vivo* and *ex vivo*, were substantially unaffected. For some aspects (mitochondrial sensitivity to submaximal [ADP]) mitochondrial function was even enhanced by bed rest. An unexpected and interesting observation was represented by the decreased resting $\dot{V}\text{O}_2m$ after bed rest.

Microvascular–endothelial function was evaluated by the method recently proposed by Gifford and Richardson (2017). The blood flow increase (determined by Doppler ultrasound) in the common femoral artery during a 1 min period of passive knee flexion–extension (PLM) has been determined in young untrained and trained subjects, untrained and trained older adults, patients with chronic heart failure (Gifford & Richardson, 2017) and patients with chronic obstructive pulmonary disease (Ives *et al.* 2020). The blood flow increase during PLM was higher in trained *vs.* untrained subjects, higher in young *vs.* old subjects, lower in patients *vs.* healthy controls. Moreover, the blood flow increase during PLM was well correlated with indices of nitric oxide availability and endothelial function (Gifford & Richardson, 2017), a critical index of general cardiovascular health. According to Gifford & Richardson (2017), although the PLM-induced response is measured in the common femoral artery, its strong relationship with

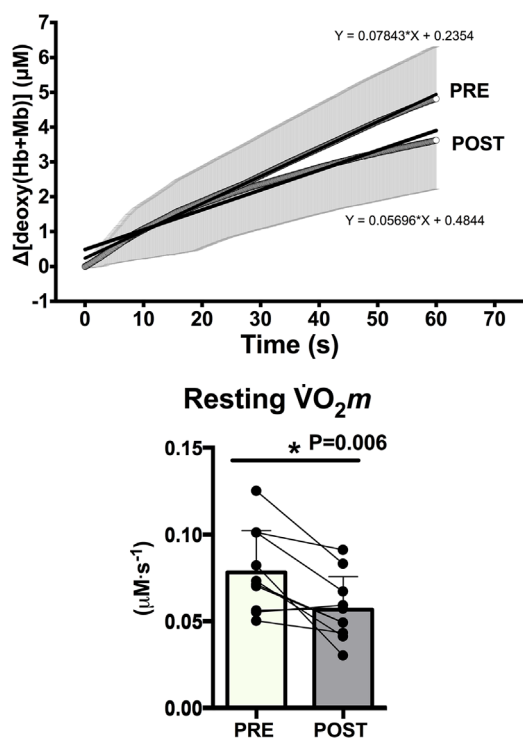


Figure 5. Resting muscle $\dot{V}\text{O}_2m$

In the upper panel mean linear regression lines of the $\Delta[\text{deoxy}(\text{Hb} + \text{Mb})]$ increase during the first minute of the blood occlusion manoeuvres performed for the ‘physiological calibration’ (see *Methods*) are presented; data were obtained before (PRE) and after (POST) bed rest. The equations describing the linear regression lines are also given in the figure. In the lower panel individual and mean (\pm SD) values of resting muscle $\dot{V}\text{O}_2m$ ($\dot{V}\text{O}_2m$), estimated by NIRS before (PRE) and after (POST) bed rest, are shown. * indicates the presence of a statistically significant difference. See text for further details. [Colour figure can be viewed at wileyonlinelibrary.com]

acetylcholine-induced dilatation of the microvasculature, a common marker of microvascular function, points to a more distal site of functional evaluation compared with flow-mediated vasodilation (FMD), classically considered a biomarker of conduit artery function.

In our study we observed a less pronounced blood flow increase during PLM after 10 days of bed rest (see Fig. 1), suggesting an early impairment of microvascular/endothelial function following simulated microgravity-inactivity. Interestingly, the blood flow increase during PLM observed in our young subjects after 10 days of bed rest was not substantially different from that described by Gifford and Richardson (2017) in subjects of 60–70 years of age. Moreover, the less pronounced increase in blood flow during PLM after bed rest was associated with a reduction of the common femoral artery lumen diameter. In the present study, 10 days of bed rest led to a 5% decrease (0.5 mm) in resting lumen diameter of the vessel. A very similar decrease (6%) was detected after 7 days of leg casting (Sugawara *et al.* 2004). This phenomenon has also been reported across a spectrum of different modalities of physical inactivity, ranging from spinal cord injury patients, bed rest and unilateral lower limb suspension (Thijssen *et al.* 2011). Changes in femoral artery diameter are also associated with increases in wall thickness, with the result of promoting atherosclerotic progression (Thijssen *et al.* 2011). A decreased leg blood flow was described before following a short period of bed rest (Mikines *et al.* 1991).

In the present study, microvascular function was evaluated by also utilizing another biomarker, related to the intramuscular matching between O₂ delivery and O₂ uptake. A critical issue of peripheral oxidative metabolism, particularly during metabolic transitions

(rest-to-exercise, lower-to-higher intensity exercise), deals with the temporal and spatial intramuscular matching between O₂ delivery and O₂ uptake (Grassi *et al.* 2019), in which nitric oxide plays a critical role (Poole *et al.* 2012). A ‘weak spot’ in this matching resides in the very different morphological and functional organization of muscle fibre recruitment, based upon the motor unit, and of microvascular recruitment, based upon the ‘microvascular unit’ (Segal 1999). During metabolic transitions a suboptimal intramuscular matching between O₂ delivery and O₂ uptake could lead to a transient underperfusion of areas of muscles, and possibly to a transient overperfusion of other regions. The resulting O₂ delivery-to-O₂ uptake mismatch could determine a transiently increased (‘overshoot’) microvascular fractional O₂ extraction, which has been repeatedly demonstrated by NIRS in pathological conditions (Porcelli *et al.* 2014, 2016; Grassi *et al.* 2019), as well as in subjects exposed to bed rest periods of longer duration (Porcelli *et al.* 2010, Salvadego *et al.* 2018). The overshoot of fractional O₂ extraction would represent a ‘mirror image’ of the undershoot of microvascular O₂ partial pressure (PO₂) described by phosphorescence quenching (Poole *et al.* 2012). A lowering of microvascular PO₂, albeit transitory, would decrease O₂ driving pressure for blood to myocyte O₂ flux, thereby impairing peripheral O₂ diffusion and skeletal muscle oxidative metabolism.

In the present study the intramuscular matching between O₂ delivery and O₂ uptake was evaluated by analysing the dynamic profiles of [deoxy(Hb + Mb)] during the first 60 s of low-intensity constant work rate cycling exercise, as previously described (Porcelli *et al.* 2010, 2014, 2016; Salvadego *et al.* 2018). After 10 days of horizontal bed rest, the time-course of [deoxy(Hb + Mb)] was characterized by a greater transient overshoot

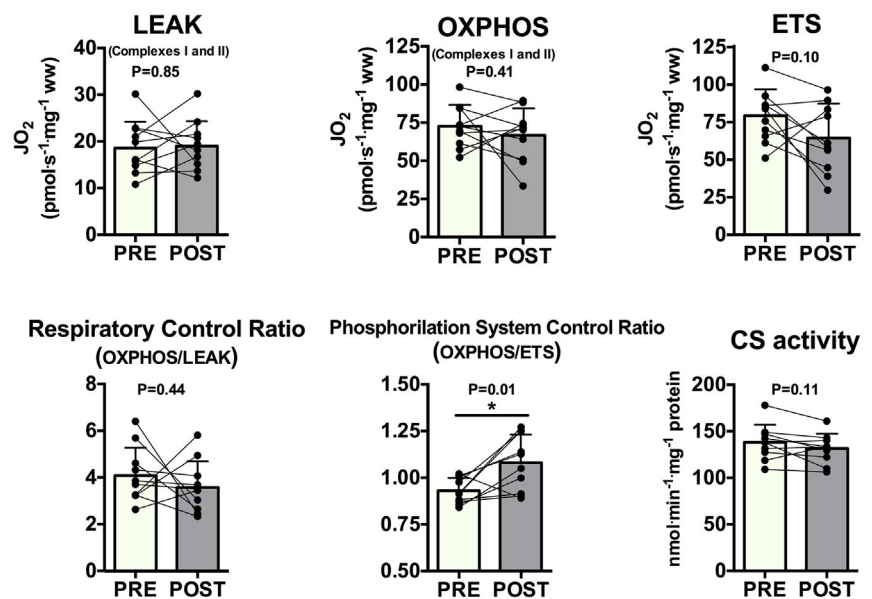


Figure 6. Assessments of *ex vivo* mitochondrial function and mass
Individual and mean (\pm SD) values of mitochondrial respiration variables obtained by high-resolution respirometry in permeabilized skeletal muscle fibres are shown; data were obtained before (PRE) and after (POST) bed rest. In the upper panel: LEAK respiration, OXPPOS capacity, and electron transport system (ETS) capacity. In the lower panel: respiratory control ratio (OXPPOS/LEAK) and citrate synthase (CS) activity. No statistically significant differences were observed. See text for further details. [Colour figure can be viewed at wileyonlinelibrary.com]

compared with measurements before bed rest, implying an impaired matching between intramuscular O₂ delivery and metabolic demand. This microvascular impairment therefore appears to be in agreement with that identified by the PLM approach described above, and definitively points to a microvascular impairment following 10 days of bed rest.

Mitochondrial function evaluated by high-resolution respirometry on isolated and permeabilized non-contracting skeletal muscle fibres (Perry *et al.* 2011; Pesta & Gnaiger 2012), showed similar results to those observed by Salvadego *et al.* (2016): no variables were affected by bed rest (see Fig. 6). ‘Leak’ respiration, which represents the dissipation of the H⁺ gradient across the inner mitochondrial membrane, not associated with phosphorylation of ADP, was not different following bed rest. Maximal ADP-stimulated mitochondrial respiration (OXPHOS) supported by complex I and complex II, determined in the presence of saturating ADP levels and unlimited substrates and O₂ availability, was unchanged as well. Also, the maximal capacity of electron transport system (ETS), uncoupled from the phosphorylating

system, the rotenone-insensitive ETS and oxidative phosphorylation coupling were not affected. Interestingly, the uncoupled mitochondrial respiration was significantly higher than oxidative phosphorylation capacity only before bed rest (see Fig. 6). An increased oxygen flux following the uncoupling of mitochondrial respiration is expected to occur in skeletal muscle fibres when the phosphorylation system (i.e. adenine nucleotide translocase, ANT, phosphate carrier and ATP synthase) limits OXPHOS capacity (Pesta & Gnaiger 2012). In the present study it seems that following bed rest the capacity of the phosphorylation pathway fully matches ETS capacity, such that OXPHOS capacity was not limited by the phosphorylation system or by the proton backpressure. This phenomenon typically occurs in mouse skeletal and cardiac tissue (Gnaiger *et al.* 2009; Lemieux *et al.* 2017). Further investigations are needed to clarify the mechanisms responsible for these observations.

The absence of significant differences was also confirmed after the respirometric data were normalized per unit of CS activity, taken as an index of mitochondrial mass (Larsen *et al.* 2012), which was not affected by bed rest either. In previous studies, the effects of short periods of bed rest on maximal ADP-stimulated mitochondrial respiration are somehow controversial. Whereas Miotto *et al.* (2019) and Dirks *et al.* (2020) described an impaired mitochondrial function following bed rest periods of 3 and 7 days, respectively, other authors (Salvadego *et al.* 2016; Larsen *et al.* 2018) did not see impairments following 4 and 10 days of bed rest. No hypotheses can be forwarded to explain the conflicting data. It should be mentioned that in the present study the absence of differences of mitochondrial respiration following bed rest was also confirmed by the biomarker obtained *in vivo* (see below). According to data obtained by a different group belonging to the present project (Sandri *et al.*, unpublished observations) a substantial impairment of the ‘transcriptome’ of mitochondrial genes occurs as early as after 5 days of bed rest. The contradiction with our results, however, could be only apparent, in the sense that changes at the level of the transcriptome may become evident before functional changes are observed. The scenario could be different with a more prolonged exposure to simulated microgravity, a condition in which both respirometric (Salvadego *et al.* 2018) and proteomic data (Brocca *et al.* 2012; Buso *et al.* 2019) are in favour of altered mitochondrial function and structure.

In the present study we also investigated the sensibility of mitochondrial respiration to submaximal (and physiological) [ADP]. Free [ADP] in skeletal muscle ranges between 25 and 250 μM (Howlett *et al.* 1998), way below the unlimiting [ADP] utilized to evaluate maximal ADP-stimulated mitochondrial respiration (OXPHOS). In the present study we utilized increasing [ADP], starting from 12.5 μM, thereby including also

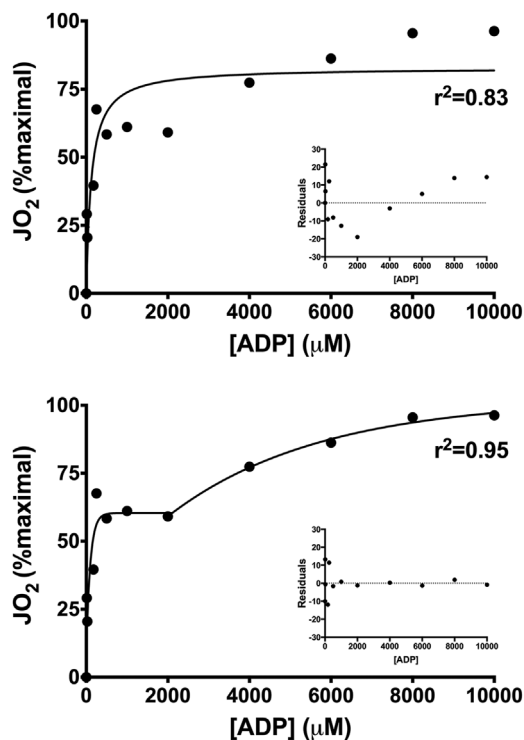


Figure 7. Mitochondrial ADP sensitivity

The two graphs show the ADP-stimulated mitochondrial respiration data (JO₂, expressed as a percentage of maximal values) in a typical subject. In the upper panel, data are fitted according to a Michaelis–Menten kinetics curve, whereas in the lower panel the same data are fitted by a double exponential model (see *Methods*). The double exponential model increases the quality of the fitting, as also confirmed by the analysis of residuals (see inserts). See text for further details.

'physiological' [ADP] values. The parameter equivalent to the apparent K_m ([ADP] at 50% of JO_2 max) was estimated by solving a biexponential function, which provided a better fit of experimental data compared with the traditional fitting for K_m estimation according to Michaelis–Menten kinetics (see Fig. 7). Analysis of previous studies which applied the Michaelis–Menten kinetics model (see, e.g. Perry *et al.* 2011; Holloway *et al.* 2018) to fit JO_2 vs. [ADP] data confirms the unsatisfactory fitting. At the moment we do not know if the new fitting we are proposing represents only a mathematical improvement, or if it can give insights into cellular mechanisms regulating mitochondrial respiration, possibly related to the presence of different fibres with different respiratory sensitivity to [ADP], and/or to the presence of multiple regulatory factors. The measured JO_2 in the presence of ADP represents indeed the final product of complex reactions, and not a single reaction. These complex reactions involve at least four components: transport of nucleotides across external and internal mitochondrial membrane, transport of phosphate, ATP synthase activity and respiratory chain activity (Mitchell & Moyle, 1967; Guzun *et al.* 2012; Letts & Sazaov, 2017).

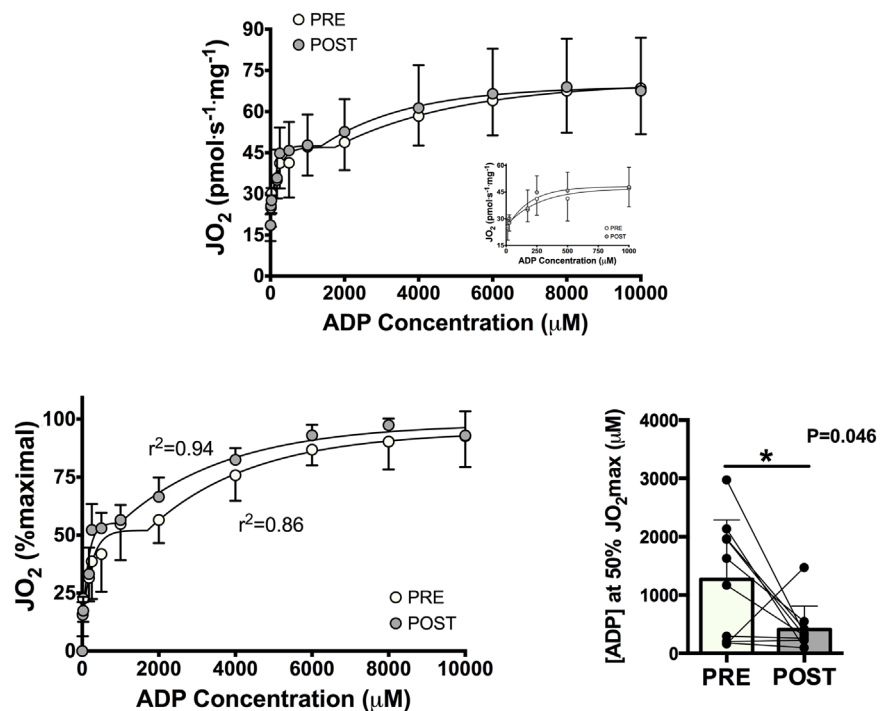
In any case, in the present study, whereas maximal ADP-stimulated mitochondrial respiration and other respirometric variables remained unchanged after bed rest, sensitivity of mitochondrial respiration to sub-maximal [ADP] was enhanced, as shown by the leftward shift of the JO_2 vs. [ADP] relationship (higher JO_2 for the same [ADP] after bed rest) and by the lower values

of [ADP] at a JO_2 corresponding to 50% of max. A conclusive interpretation of these data is still lacking, but they are in accordance with literature findings, showing a decrease in ADP sensitivity (higher K_m) of skeletal muscle fibres following training (Walsh *et al.* 2001). The present data also confirm the results obtained by Dirks *et al.* (2020) following a bed rest period of similar duration. In that study the observation was associated with a reduction in OXPHOS protein content, but with an unchanged content of proteins involved in the transport of ADP across the outer (voltage-dependent anion channel, VDAC) and inner (adenine nucleotide translocase, ANT) mitochondrial membranes (Dirks *et al.* 2020). Considering that we observed no reduction in either mitochondrial mass (CS activity) or state III respiration, no reduction in protein content should be involved of either OXPHOS and mitochondrial proteins involved in ADP transport across the outer (i.e. VDAC) and inner (i.e. ANT) membranes. Conversely, we can postulate that post-translational modifications/functional regulation of mitochondrial membrane transporters are the more likely to be responsible for the effect. Further investigations are needed to verify such a tempting hypothesis. The reduced apparent K_m after bed rest could be interpreted as an attempt to maintain metabolic homeostasis (Dirks *et al.* 2020) in the presence of impairments upstream of mitochondria, as discussed above.

In the present study, mitochondrial mass, as estimated by CS activity, was not affected by bed rest. Also in quantitative terms, therefore, mitochondria were not

Figure 8. Assessments of mitochondrial ADP sensitivity

Top panel: ADP-stimulated mitochondrial respiration values (JO_2 , expressed as absolute values) before (PRE) and after (POST) bed rest; an enlargement of the graph showing the first six ADP titrations is shown in the insert. Data are presented as means \pm SD. The fittings with the double exponential model (see *Methods*) are also shown. The curves in POST are shifted to the left compared with the curves in PRE. Bottom left panel: individual and mean relative values (\pm SD) of ADP-stimulated mitochondrial respiration values (JO_2 , expressed as a percentage of maximal values). Bottom right panel: variable corresponding to the apparent K_m for a Michaelis–Menten kinetics ([ADP] values corresponding to 50% JO_2 max). * indicates the presence of a statistically significant difference. See text for further details. [Colour figure can be viewed at wileyonlinelibrary.com]



affected. This observation confirms previous observations by our group and others following a relatively short bed rest period (Salvadego *et al.* 2016; Dirks *et al.* 2020), but it is in disagreement with other observations in which CS activity was reduced after 4 and 7 days of bed rest (Dirks *et al.* 2016; Larsen *et al.* 2018). With prolonged periods of bed rest, mitochondrial mass was reduced after 4 weeks and 42 days of bed rest (Berg *et al.* 1993; Ferretti *et al.* 1997).

The absence of impairments of mitochondrial respiration, observed *ex vivo* by high-resolution respirometry on isolated skeletal muscle fibres, was also confirmed *in vivo*, non-invasively, by the analysis of the kinetics of $\dot{V}O_{2m}$ recovery following cycle ergometer exercise, carried out by NIRS and the repeated occlusions method (Ryan *et al.* 2012; Adami & Rossiter, 2018; Zuccarelli *et al.* 2020). $\dot{V}O_{2m}$ recovery kinetics is a mirror image of phosphocreatine recovery kinetics (Ryan *et al.* 2013), which is considered a classic evaluation tool for intramuscular oxidative metabolism (Kent & Fitzgerald, 2016). Methodological improvements in the method adopted in the present study, with respect to the conventional approach (Ryan *et al.* 2012, Adami & Rossiter, 2018), are discussed in detail in a previous study by our group (Zuccarelli *et al.* 2020). To the best of our knowledge, this is the first time that this methodology has been applied after bed rest. The time constant (τ) of $\dot{V}O_{2m}$ recovery kinetics was not affected by bed rest (see Fig. 4), thus confirming that skeletal muscle mitochondrial function was not compromised.

An unexpected and interesting finding of the present study is related to the resting $\dot{V}O_{2m}$, measured non-invasively by calculating the linear slope of muscle deoxygenation (determined by NIRS) during a transitory limb ischaemia induced by the rapid inflation of a pneumatic cuff. A significant decrease (of about 25%) in resting $\dot{V}O_{2m}$ was observed following bed rest. A decrease in whole body resting $\dot{V}O_2$ of about 7% after 7 weeks of immobilization has been reported by Deitrick *et al.* (1948), and it was subsequently confirmed by other studies (Teasell & Dittmer, 1993; Downs *et al.* 2020). No similar data are available for immobilization periods of shorter duration. Disuse/immobilization is known to decrease muscle protein synthesis and increase muscle protein degradation, leading to skeletal muscle atrophy (Crossland *et al.* 2019; Degens *et al.* 2019). Data obtained by other groups of the present research project indicate a decrease in quadriceps femoris volume by about 5% (Monti *et al.* 2021). As far as we know, the present data are the first to demonstrate a decreased resting $\dot{V}O_{2m}$ induced by bed rest. Anabolic reactions in muscle are energetically more expensive than catabolic ones. Thus, a reduction of muscle protein synthesis, even in the presence of an enhanced protein degradation, would decrease the energy expenditure in resting muscle. It is noteworthy that the

decreased resting energy expenditure in skeletal muscle was quantitatively significant (-25%) after only 10 days of bed rest. It would be of interest to determine this variable after longer bed rest periods. It is intriguing to note, in this respect, that a state of 'metabolic depression' (about a 20% decrease of metabolic rate relative to basal levels) has been recently proposed as a condition mitigating the biological and logistical challenges of human spaceflight (Regan *et al.* 2020).

The reduction in resting $\dot{V}O_{2m}$ observed in the present study could also be the result of a higher muscle oxidative phosphorylation efficiency at rest (i.e. lower O_2 cost of ATP resynthesis). In this regard, however, no changes in leak mitochondrial respiration or in the respiratory control ratio were detected in the present study, suggesting that immobilization plays a role in decreasing energy expenditure at rest, rather than increasing muscle mitochondrial efficiency.

The decreased resting $\dot{V}O_{2m}$ observed in the present study after bed rest cannot be attributed to muscle atrophy. The volume of the small and superficial area of muscle investigated by the NIRS probe (Grassi & Quaresima, 2016) is indeed the same, irrespective of muscle atrophy. If anything, the small decrease in ATT observed after bed rest would increase the relative proportion of muscle *vs.* adipose tissue investigated by the probe. Since energy turnover in skeletal muscle tissue is greater than that in adipose tissue, this would go in the direction of underestimating the observed resting $\dot{V}O_{2m}$ decrease after bed rest.

Some limitations are present in the study: (i) no analysis of relevant protein involved in both oxidative metabolism and angiogenic processes and capillarization have been performed; (ii) respirometric measurements were not extended to mitochondrial-derived reactive oxygen species production; and (iii) resting muscle $\dot{V}O_2$ measurements, estimated by NIRS during transient ischaemic periods, were not corroborated by other independent measurements, such as resting energy expenditure.

In conclusion, the main peripheral limitations to oxidative metabolism after a 10-day horizontal bed rest were 'upstream' of mitochondrial function, at the level of microvascular O_2 delivery. Substantial impairments were observed for biomarkers of microvascular/endothelial function, and for the intramuscular matching between O_2 delivery and O_2 uptake. On the other hand, mitochondrial content and mitochondrial respiration were unaffected or even improved (i.e. enhanced mitochondrial sensitivity to submaximal [ADP]) following bed rest. An unchanged mitochondrial respiration was also confirmed by a biomarker obtained *in vivo* ($\dot{V}O_{2m}$ recovery kinetics). The decreased resting $\dot{V}O_{2m}$ (by about 25%) following bed rest could represent an adaptive phenomenon in response to simulated microgravity-inactivity,

attributable to the fact that muscle catabolic processes within muscles are less expensive, in terms of energy, than anabolic ones. The concepts mentioned above, besides being of interest from a basic science point of view, may be relevant for pathological conditions characterized by relatively short periods of profound inactivity, and they could affect the definition of countermeasures or rehabilitative interventions. Future studies should be conducted in order to determine the potential causes of the interindividual variation in some physiological responses to bed rest. These studies could at least in part explain why some astronauts experience greater functional impairments in space or upon returning to Earth, and could also be useful in the selection of the astronauts.

References

- Adami A & Rossiter HB (2018). Principles, insights, and potential pitfalls of the noninvasive determination of muscle oxidative capacity by near-infrared spectroscopy. *J Appl Physiol* **124**, 245–248.
- Adami A, Cao R, Porszasz J, Casaburi R & Rossiter HB (2017). Reproducibility of NIRS assessment of muscle oxidative capacity in smokers with and without COPD. *Respir Physiol Neurobiol* **235**, 18–26.
- Ade CJ, Broxterman RM & Barstow TJ (2015). VO₂(max) and microgravity exposure: convective versus diffusive O₂ transport. *Med Sci Sports Exerc* **47**, 1351–1361.
- Ade CJ, Broxterman RM, Moore AD & Barstow TJ (2017). Decreases in maximal oxygen uptake following long-duration spaceflight: role of convective and diffusive O₂ transport mechanisms. *J Appl Physiol* **122**, 968–975.
- Barstow TJ (2019). Understanding near infrared spectroscopy and its application to skeletal muscle research. *J Appl Physiol* **126**, 1360–1376.
- Berg HE, Dudley GA, Hather B & Tesch PA (1993). Work capacity and metabolic and morphologic characteristics of the human quadriceps muscle in response to unloading. *Clin Physiol* **13**, 337–347.
- Biolo G, Agostini F, Simunic B, Sturma M, Torelli L, Preiser JC, Deby-Dupont G, Magni P, Strollo F, di Prampero P, Guarnieri G, Mekjavic IB, Pisot R & Narici MV (2008). Positive energy balance is associated with accelerated muscle atrophy and increased erythrocyte glutathione turnover during 5 wk of bed rest. *Am J Clin Nutr* **88**, 950–958.
- Booth FW, Roberts CK, Thyfault JP, Ruegsegger GN & Toedebusch RG (2017). Role of inactivity in chronic diseases: evolutionary insight and pathophysiological mechanisms. *Physiol Rev* **97**, 1351–1402.
- Brocca L, Cannavino J, Coletto L, Biolo G, Sandri M, Bottinelli R & Pellegrino MA (2012). The time course of the adaptations of human muscle proteome to bed rest and the underlying mechanisms. *J Physiol* **590**, 5211–5230.
- Buso A, Comelli M, Picco R, Isola M, Magnesa B, Pišot R, Rittweger J, Salvadego D, Šimunič B, Grassi B & Mavelli I (2019). Mitochondrial adaptations in elderly and young men skeletal muscle following 2 weeks of bed rest and rehabilitation. *Front Physiol* **10**, 474.
- Capelli C, Antonutto G, Kenfack MA, Cautero M, Lador F, Moia C, Tam E & Ferretti G (2006). Factors determining the time course of VO₂(max) decay during bedrest: implications for VO₂(max) limitation. *Eur J Appl Physiol* **98**, 152–160.
- Crossland H, Skirrow S, Puthuchery ZA, Constantin-Teodosiu D & Greenhaff PL (2019). The impact of immobilisation and inflammation on the regulation of muscle mass and insulin resistance: different routes to similar end-points. *J Physiol* **597**, 1259–1270.
- Degens H (2019). Human ageing: impact on muscle force and power. In *Muscle and exercise physiology*, ed. Zoladz JA. p. 423–432, Elsevier Academic Press, London.
- Deitrick JE, Whedon GD & Shorr E (1948). Effects of immobilization upon various metabolic and physiologic functions of normal men. *Am J Med* **4**, 3–36.
- di Prampero PE & Ferretti G (1990). Factors limiting maximal oxygen consumption in humans. *Respir Physiol* **80**, 113–128.
- Dirks ML, Miotto PM, Goossens GH, Senden JM, Petrick HL, van Kranenburg J, van Loon LJC & Holloway GP (2020). Short-term bed rest-induced insulin resistance cannot be explained by increased mitochondrial H₂O₂ emission. *J Physiol* **598**, 123–137.
- Dirks ML, Wall BT, van de Valk B, Holloway TM, Holloway GP, Chabowski A, Goossens GH & van Loon LJ (2016). One week of bed rest leads to substantial muscle atrophy and induces whole-body insulin resistance in the absence of skeletal muscle lipid accumulation. *Diabetes* **65**, 2862–2875.
- Downs ME, Scott JM, Ploutz-Snyder LL, Ploutz-Snyder R, Goetichius E, Buxton RE, Danesi CP, Randolph KM, Urban RJ, Sheffield-Moore M & Dillon EL (2020). Exercise and testosterone countermeasures to mitigate metabolic changes during bed rest. *Life Sci Space Res* **26**, 97–104.
- Ferretti G & Capelli C (2009). Maximal O₂ consumption: effects of gravity withdrawal and resumption. *Respir Physiol Neurobiol* **169**, S50–S54.
- Ferretti G, Antonutto G, Denis C, Hoppeler H, Minetti AE, Narici MV & Desplanches D (1997). The interplay of central and peripheral factors in limiting maximal O₂ consumption in man after prolonged bed rest. *J Physiol* **501**, 677–686.
- Gifford JR & Richardson RS (2017). CORP: ultrasound assessment of vascular function with the passive leg movement technique. Review: cores of reproducibility in physiology. *J Appl Physiol* **123**, 1708–1720.
- Gnaiger E (2009). Capacity of oxidative phosphorylation in human skeletal muscle: new perspectives of mitochondrial physiology. *Int J Biochem Cell Biol* **41**, 1837–1845.
- Grassi B & Quaresima V (2016). Near-infrared spectroscopy and skeletal muscle oxidative function in vivo in health and disease: a review from an exercise physiology perspective. *J Biomed Opt* **21**, 091313.
- Grassi B, Porcelli S & Marzorati M (2019). Translational medicine: exercise physiology applied to metabolic myopathies. *Med Sci Sports Exerc* **51**, 2183–2192.

- Guzun R, Gonzalez-Granillo M, Karu-Varikmaa M, Grichine A, Usson Y, Kaambre T, Guerrero-Roesch K, Kuznetsov A, Schlattner U & Saks V (2012). Regulation of respiration in muscle cells in vivo by VDAC through interaction with the cytoskeleton and MtCK within Mitochondrial Interactosome. *Biochim Biophys Acta* **1818**, 1545–1554.
- Holloway GP, Holwerda AM, Miotto PM, Dirks ML, Verdijk LB & van Loon LJC (2018). Age-associated impairments in mitochondrial ADP sensitivity contribute to redox stress in senescent human skeletal muscle. *Cell Rep* **22**, 2837–2848.
- Howlett RA, Parolin ML, Dyck DJ, Hultman E, Jones NL, Heigenhauser GJ & Spriet LL (1998). Regulation of skeletal muscle glycogen phosphorylase and PDH at varying exercise power outputs. *Am J Physiol* **275**, R418–R425.
- Ives SJ, Layec G, Hart CR, Trinity JD, Gifford JR, Garten RS, Witman MAH, Sorensen JR & Richardson RS (2020). Passive leg movement in chronic obstructive pulmonary disease: evidence of locomotor muscle vascular dysfunction. *J Appl Physiol* **128**, 1402–1411.
- Kent JA & Fitzgerald LF (2016). In vivo mitochondrial function in aging skeletal muscle: capacity, flux, and patterns of use. *J Appl Physiol* **121**, 996–1003.
- Larsen S, Lundby A-KM, Dandanell S, Oberholzer L, Keiser S, Andersen AB, Haider T & Lundby C (2018). Four days of bed rest increases intrinsic mitochondrial respiratory capacity in young healthy males. *Physiol Rep* **6**, e13793.
- Larsen S, Nielsen J, Hansen CN, Nielsen LB, Wibrand F, Stride N, Schroder HD, Boushel R, Helge JW, Dela F & Hey-Mogensen M (2012). Biomarkers of mitochondrial content in skeletal muscle of healthy young human subjects. *J Physiol* **590**, 3349–3360.
- Lemieux H, Blier PU & Gnaiger E (2017). Remodeling pathway control of mitochondrial respiratory capacity by temperature in mouse heart: electron flow through the Q-junction in permeabilized fibers. *Sci Rep* **7**, 2840.
- Letts JA & Sazanov LA (2017). Clarifying the supercomplex: the higher-order organization of the mitochondrial electron transport chain. *Nat Struct Mol Biol* **24**, 800–808.
- Lowry OH, Rosebrough NJ, Farr AL & Randall RJ (1951). Protein measurement with the Folin phenol reagent. *J Biol Chem* **193**, 265–275.
- Mikines KJ, Richter EA, Dela F & Galbo H (1991). Seven days of bed rest decrease insulin action on glucose uptake in leg and whole body. *J Appl Physiol* **70**, 1245–1254.
- Miotto PM, McGlory C, Bahniwal R, Kamal M, Phillips SM & Holloway GP (2019). Supplementation with dietary omega-3 mitigates immobilization-induced reductions in skeletal muscle mitochondrial respiration in young women. *FASEB J* **33**, 8232–8240.
- Mitchell P & Moyle J (1967). Chemiosmotic hypothesis of oxidative phosphorylation. *Nature* **213**, 137–139.
- Monti E, Reggiani C, Franchi MV, Toniolo L, Sandri M, Armani A, Zampieri S, Giacomello E, Sarto F, Sirago G, Murgia M, Nogara L, Marcucci L, Ciciliot S, Simunic B, Pisot R & Narici MV (2021). Neuromuscular junction instability and altered intracellular calcium handling as early determinants of force loss during unloading in humans. *J Physiol* **599**, 3037–3061.
- Müller MJ, Bosy-Westphal A, Klaus S, Kreyman G, Lührmann PM, Neuhäuser-Berthold M, Noack R, Pirke KM, Platte P, Selberg O & Steiniger J (2004). World Health Organization equations have shortcomings for predicting resting energy expenditure in persons from a modern, affluent population: generation of a new reference standard from a retrospective analysis of a German database of resting energy expenditure. *Am J Clin Nutr* **80**, 1379–1390.
- Pavy-Le Traon A, Heer M, Narici MV, Rittweger J & Vernikos J (2007). From space to Earth: advances in human physiology from 20 years of bed rest studies (1986–2006). *Eur J Appl Physiol* **101**, 143–194.
- Perry CG, Kane DA, Lin CT, Kozy R, Cathey BL, Lark DS, Kane CL, Brophy PM, Gavin TP, Anderson EJ & Neuffer PD (2011). Inhibiting myosin-ATPase reveals a dynamic range of mitochondrial respiratory control in skeletal muscle. *Biochem J* **437**, 215–222.
- Pesta D & Gneiger E (2012). High-resolution respirometry. OXPHOS protocols for human cell cultures and permeabilized fibers from small biopsies of human muscle. *Methods Mol Biol* **810**, 25–58.
- Poole DC, Hirai DM, Copp SW & Musch TI (2012). Muscle oxygen transport and utilization in heart failure: implications for exercise (in)tolerance. *Am J Physiol Heart Circ Physiol* **302**, H1050–H1063.
- Porcelli S, Marzorati M, Belletti M, Bellistri G, Morandi L & Grassi B (2014). The ‘second wind’ in McArdle’s disease patients during a second bout of constant work rate sub-maximal exercise. *J Appl Physiol* **116**, 1230–1237.
- Porcelli S, Marzorati M, Lanfranconi F, Vago P, Pisot R & Grassi B (2010). Role of skeletal muscles impairment and brain oxygenation in limiting oxidative metabolism during exercise after bed rest. *J Appl Physiol* **109**, 101–111.
- Porcelli S, Marzorati M, Morandi L & Grassi B (2016). Home-based aerobic exercise training improves skeletal muscle oxidative metabolism in patients with metabolic myopathies. *J Appl Physiol* **121**, 699–708.
- Regan MD, Flynn-Evans EE, Griko YV, Kilduff TS, Rittenberger JC, Ruskin KJ & Buck CL (2020). Shallow metabolic depression and human spaceflight: a feasible first step. *J Appl Physiol* **128**, 637–647.
- Richardson RS, Poole DC, Knight DR, Kurdak SS, Hogan MC, Grassi B, Johnson EC, Kendrick KF, Erickson BK & Wagner PD (1993). High muscle blood flow in man: is maximal O₂ extraction compromised? *J Appl Physiol* **75**, 1911–1916.
- Ried-Larsen M, Aarts HM & Joyner MJ (2017). Effects of strict prolonged bed rest on cardiorespiratory fitness: systematic review and meta-analysis. *J Appl Physiol* **123**, 790–799.
- Ryan TE, Brophy P, Lin CT, Hickner RC & Neuffer PD (2014). Assessment of in vivo skeletal muscle mitochondrial respiratory capacity in humans by near-infrared spectroscopy: a comparison with in situ measurements. *J Physiol* **592**, 3231–3241.
- Ryan TE, Erickson ML, Brizendine JT, Young HJ & McCully KK (2012). Non-invasive evaluation of skeletal muscle mitochondrial capacity with near-infrared spectroscopy: correcting for blood volume changes. *J Appl Physiol* **113**, 175–183.

- Ryan TE, Southern WM, Reynolds MA, McCully KK (2013). A cross-validation of near-infrared spectroscopy measurements of skeletal muscle oxidative capacity with phosphorus magnetic resonance spectroscopy. *J Appl Physiol* **115**, 1757–1766.
- Saltin B, Blomqvist G, Mitchell JH, Johnson RL Jr, Wildenthal K & Chapman CB (1968). Response to exercise after bed rest and after training. *Circulation* **38**, 1–78.
- Salvadego D, Keramidas ME, Brocca L, Domenis R, Mavelli I, Rittweger J, Eiken O, Mekjavic IB & Grassi B (2016). Separate and combined effects of a 10-d exposure to hypoxia and inactivity on oxidative function in vivo and mitochondrial respiration ex vivo in humans. *J Appl Physiol* **121**, 154–163.
- Salvadego D, Keramidas ME, Kölegård R, Brocca L, Lazzar S, Mavelli I, Rittweger J, Eiken O, Mekjavic IB & Grassi B (2018). PlanHab*: hypoxia does not worsen the impairment of skeletal muscle oxidative function induced by bed rest alone. *J Physiol* **596**, 3341–3355.
- Salvadego D, Lazzar S, Marzorati M, Porcelli S, Rejc E, Simunic B, Pisot R, di Prampero PE & Grassi B (2011). Functional impairment of skeletal muscle oxidative metabolism during knee extension exercise after bed rest. *J Appl Physiol* **111**, 1719–1726.
- Segal SS (1999). Chapter 11. Dynamics of microvascular control in skeletal muscle. In *Exercise and circulation in health and disease*, ed. Saltin B, Boushel R, Secher N & Mitchell JH, p. 141–153, Champaign: Human Kinetics.
- Spinazzi M, Casarin A, Pertegato V, Salviati L & Angelini C (2012). Assessment of mitochondrial respiratory chain enzymatic activities on tissues and cultured cells. *Nat Protoc* **7**, 1235–1246.
- Srere PA (1969). Citrate synthase. *Methods Enzymol* **13**, 3–11.
- Sugawara J, Hayashi K, Kaneko F, Yamada H, Kizuka T & Tanaka H (2004). Reductions in basal limb blood flow and lumen diameter after short-term leg casting. *Med Sci Sports Exerc* **36**, 1689–1694.
- Teasell R & Dittmer DK (1993). Complications of immobilization and bed rest. Part 2: other complications. *Can Fam Physician* **39**, 1440–1442, 1445–1446.
- Tijssen DH, Green DJ & Hopman MT (2011). Blood vessel remodeling and physical inactivity in humans. *J Appl Physiol* **111**, 1836–1845.
- Wagner PD (1993). Algebraic analysis of the determinants of $\dot{V}O_2$ max. *Respir Physiol* **93**, 221–237.
- Walsh B, Tonkonogi M & Sahlin K (2001). Effect of endurance training on oxidative and antioxidative function in human permeabilized muscle fibres. *Pflugers Arch* **442**, 420–425.
- Zuccarelli L, do Nascimento Salvador PC, Del Torto A, Fiorentino R & Grassi B (2020). Skeletal muscle $\dot{V}O_2$ kinetics by the NIRS repeated occlusions method during the recovery from cycle ergometry exercise. *J Appl Physiol* **128**, 534–544.

Additional information

Data availability statement

All relevant data are presented as individual data points in the figures. Data not presented with individual data points are available from the corresponding author upon request.

Competing interests

No competing interest are declared.

Author contributions

B.G. and M.N. conceived the study and obtained the financial support. B.S. and R.P. were responsible for the organization of the bed rest campaign. B.G., L.Z. and L.R. contributed to the experimental design. L.Z., G.B., B.M., C.D., M.G., G.M., M.M., A.P., S.P. and L.R. collected the data. L.Z., G.B., B.M., C.D., G.M. and B.G. analysed the data. M.C. and I.M. contributed to the *ex vivo* mitochondrial respiration analysis. L.Z. and B.G. wrote the original draft. All authors critically revised the draft and approved the final version of the manuscript.

Funding

This work was supported by the Italian Space Agency (ASI, MARS-PRE Project, Grant No. DC-VUM-2017-006).

Acknowledgements

The authors thank the volunteers who enthusiastically participated in the bed rest campaign, the support staff, the nurses and the medical personnel of the hospital ward (Splošna Bolnišnica Izola, Izola, Slovenia) where the bed rest campaign was carried out. The authors also thank Drs Jerzy Zoladz, Massimo Venturelli, Luigi Vetrugno, Robert C.W. Wust, Giovanna Lippe and Paolo Bernardi for constructive criticism.

Open Access Funding provided by Università degli Studi di Udine within the CRUI-CARE Agreement.

Keywords

bed rest, microgravity, mitochondrial respiration, NIRS, oxidative metabolism, PLM, skeletal muscle

Supporting information

Additional supporting information can be found online in the Supporting Information section at the end of the HTML view of the article. Supporting information files available:

Peer Review History Statistical Summary Document